Supplement to September / October 2024
Volume 53, Number 5

AppliedRadiology®

The Journal of Practical Medical Imaging and Management

Pediatric Imaging Case Series

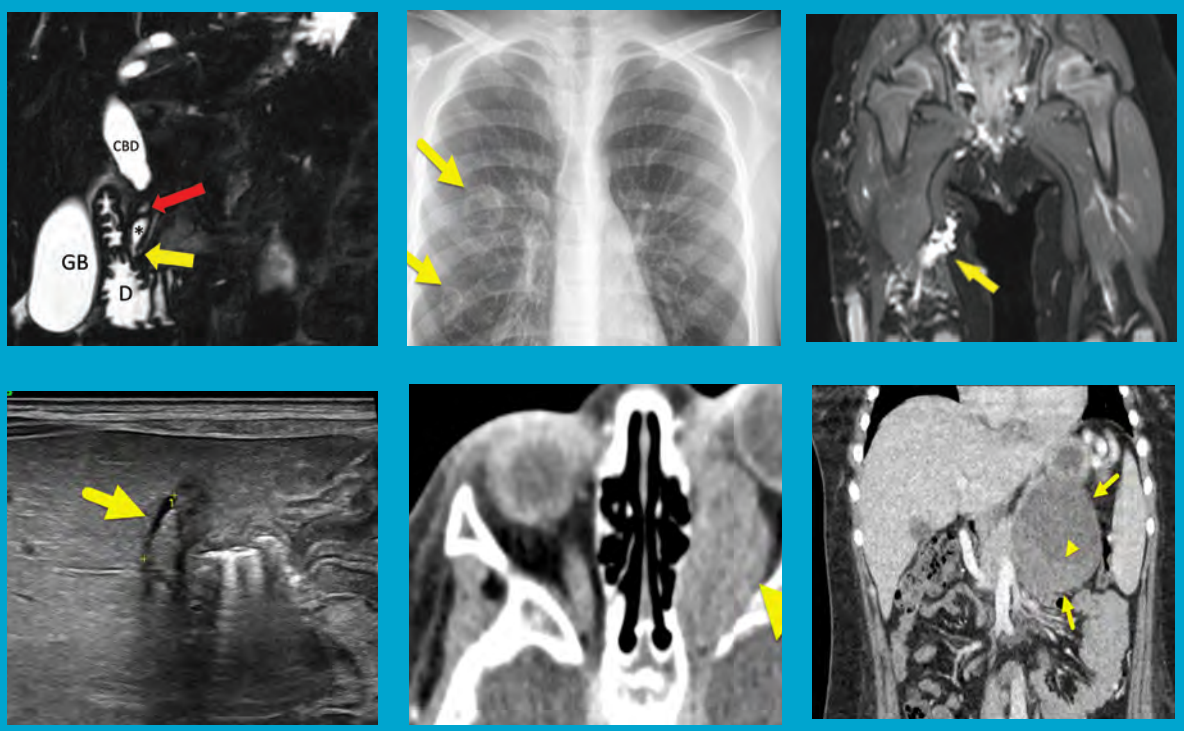

Cystic Biliary Artresia| Recurrent Respiratory Papillomatosis| Klippel-Trenaunay Syndrome
Orbital Rhabdoid Tumor | Pancreatic Divisum in Children
Solid Pseudopapillary Tumor of the Pancreas

Applied Radiology®

The Journal of Practical Medical Imaging and Management

Anderson Publishing, Ltd
180 Glenside Avenue,
Scotch Plains, NJ 07076
Tel: 908-301-1995
Fax: 908-301-1997
info@appliedradiology.com

Contents

Cystic Biliary Atresia

Brandon G. O'Connor, DO; Richard B. Towbin, MD; Carrie M. Schaefer, MD; Alexander J. Towbin, MD

Case Summary

An infant born at 33 weeks' gestation presented with neonatal cholestasis. Total and direct bilirubin levels were significantly elevated. The patient's stool color was normal. Mild jaundice and scleral icterus were found on examination.

Imaging Findings

Ultrasound (US, Figure 1) showed a 1 mm × 8-mm atretic gallbladder, despite the infant having nothing by mouth for 5 hours prior to the study. There were no visible intrahepatic bile ducts. Additionally, a 5 × 4-mm cyst was present near the hepatic hilum.

MRI cholangiopancreatography (MRCP) (Figure 2) confirmed gallbladder atresia and the cyst in the hepatic hilum. The common bile duct was not visible.

Intraoperative cholangiogram (Figure 3) showed filling of the cystic structure but no contrast within intrahepatic bile ducts or draining into the duodenum.

Diagnosis

Cystic biliary atresia.

Differential diagnosis includes choledochal cyst and Alagille syndrome.

Discussion

Biliary atresia is a progressive congenital disease involving sclerosing inflammation and obstruction of the intra- and extrahepatic bile ducts.[1,2] While it is the most common cause of cirrhosis and hepatic failure in children, its incidence varies by region. BA is most common in Taiwan, where it affects 1 in 5000 live births, and least common in the Netherlands, where it affects 1 in 19,000 live births.[2-4] Patients typically present with jaundice, pale-colored stool, dark urine, coagulopathy, and failure to thrive. Chronic findings include cirrhosis, hepatosplenomegaly, and ascites.[3]

BA is classified according to the most proximal level of the biliary obstruction. In type 1 BA (~5% of patients), the biliary system is patent to the level of the proximal common bile duct at the cystic duct insertion. There is atresia of distal common bile duct. In type 2 BA (~2% of patients), the common hepatic duct is atretic, but intrahepatic ducts are patent and cystic ducts can be found at the porta hepatis. In type 2A, the common bile duct is patent while in type 2B the cystic ducts and hepatic ducts are not patent. Finally, in type 3 BA (~90% of patients), the central intrahepatic ducts and the extrahepatic biliary are atretic.[1,3] Cystic biliary atresia (CBA) is an uncommon variant of BA accounting for 5% to 10% of patients with BA.[1] CBA is characterized by bile duct atresia, with cystic changes in the common hepatic or common bile duct.[1]

Abdominal US is the initial imaging modality in patients with suspected BA. In children younger than 1 year, a healthy gallbladder should measure 15 to 30 mm in length and should have thin, defined walls.[5] Patients with BA may have findings known as the gallbladder "ghost triad," with a gallbladder less than 19 mm in length with a thin, indistinct wall and an irregular or lobulated contour.[5] Nonvisualization of the gallbladder alone on US cannot confirm BA.[5] Other than gallbladder abnormalities, additional US findings of BA include triangular cord sign, absence/nonvisibility of the common bile duct, and hepatic artery enlargement.[1-5] The triangular cord sign represents a triangular or tubular echogenic cord of fibrous tissue more than 4 mm in thickness along the anterior wall of the right portal vein, representing an obliterated bile duct.[2,5] Prior studies have shown that a hepatic artery diameter greater than or equal to

Affiliations: University of the Incarnate Word School of Osteopathic Medicine, San Antonio, Texas (O'Connor); Department of Radiology, Phoenix Children's Hospital, Phoenix, Arizona (RB Towbin, Schaefer); Cincinnati Children's Hospital, University of Cincinnati College of Medicine, Cincinnati, Ohio (AJ Towbin).

Published: October 1, 2024. https://doi.org/10.1016/10.37549/AR-D-24-0018

Figure 1. US of the liver showed an atretic gallbladder (A, arrow) 8 mm in length and 1 mm in diameter. A 5 mm cyst (B, calipers) was present at the hepatic hilum. The common bile duct (C) was not definitively identified. However, a candidate duct (arrow) was 0.4 mm in diameter. There was a small triangular cord sign (D, arrow), 2 mm in diameter.

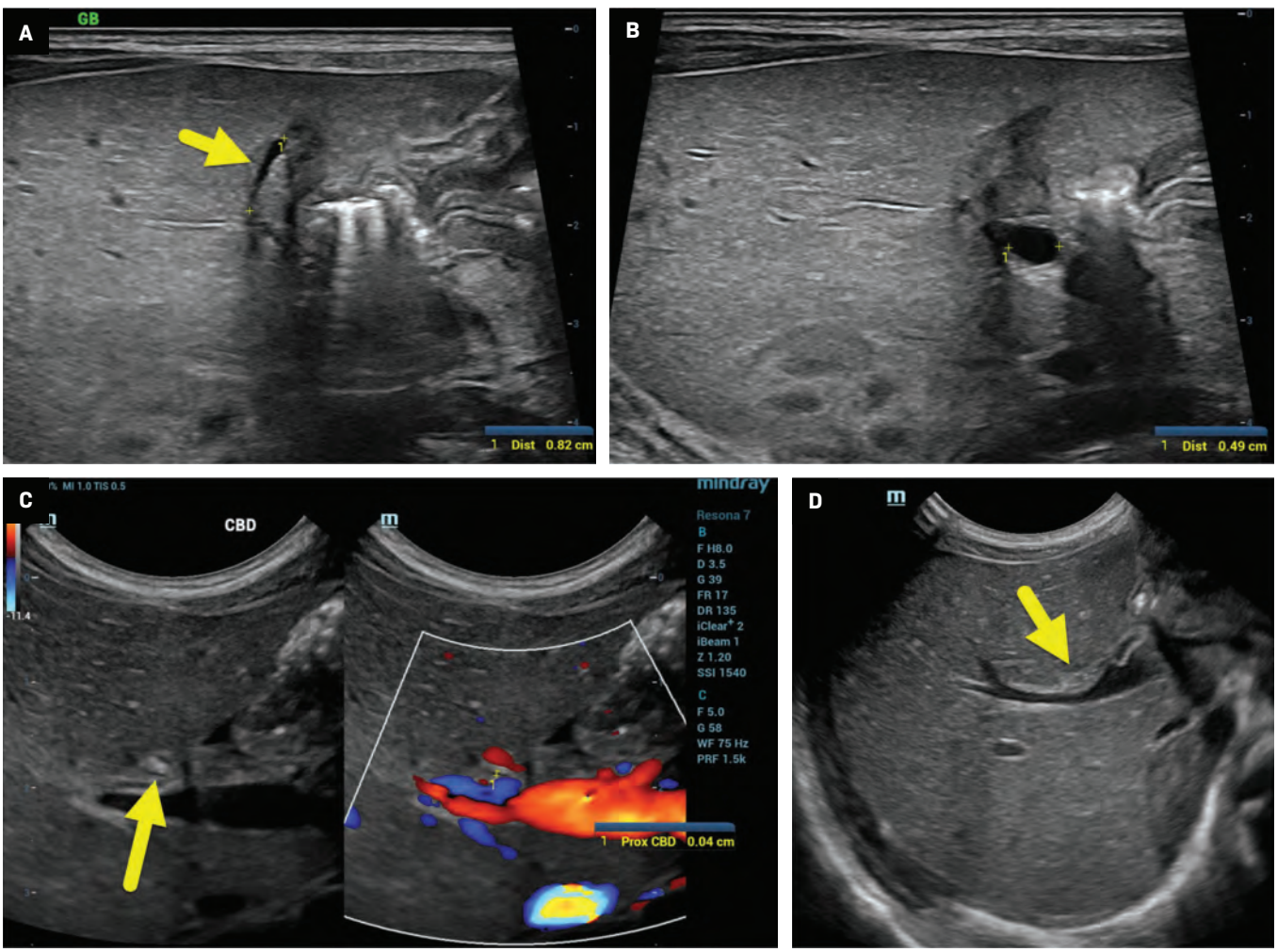

1.5 mm has a high sensitivity, specificity, and accuracy for BA.[5]

Although abdominal US is the primary imaging modality used to evaluate BA, an MRI, MRCP, nuclear medicine hepatobiliary iminodiacetic acid (HIDA) scan, and cholangiography may also be used for diagnosis. MRI and MRCP are more commonly used to exclude other causes of cholestasis.[5] MRI and MRCP findings in patients with BA are similar to US findings. When using MRI, findings for BA are triangular cord thickness greater than or equal to 5.1 mm, nonvisualization of the common bile duct, and abnormal gallbladder.[5] During HIDA scans, an injected hepatobiliary agent is taken up by hepatocytes. If the radiotracer does not excrete into the small bowel after 24 hours, a diagnosis of BA can be suggested.[5] However, neonatal hepatitis can have similar HIDA scan findings. Percutaneous or intraoperative cholangiogram may also be performed. The findings of BA include failure of contrast to opacify into the intrahepatic and extrahepatic bile ducts .[5]

BA is ultimately diagnosed via biopsy. An adequate liver biopsy should be at least 2.0 cm long × 0.2 mm wide, and ideally contain at least 10 portal areas.[6] In BA, the liver has expanded, edematous myofibroblastic portal tracts with bile duct proliferation and anastomosing ductules at the periphery of the portal tracts.[6] Ductular bile plugs, fibroblast proliferation, and inflammatory cells, particularly neutrophils, are characteristic on histopathology.[6] In CBA, the cyst has a thin, uniform layer of dense scar tissue with very few cells that tend

Figure 2. Coronal imaging (A) from MRCP and axial (B) and coronal T2-weighted images (C) showed a small cyst (arrow) at the hepatic hilum. There were no visible gallbladder or intrahepatic bile ducts. Axial T2-weighted imaging (D) near the portal bifurcation (arrow) showed increased signal related to inflammation, with no visible bile ducts. Note the diffuse, low T2 signal throughout the liver.

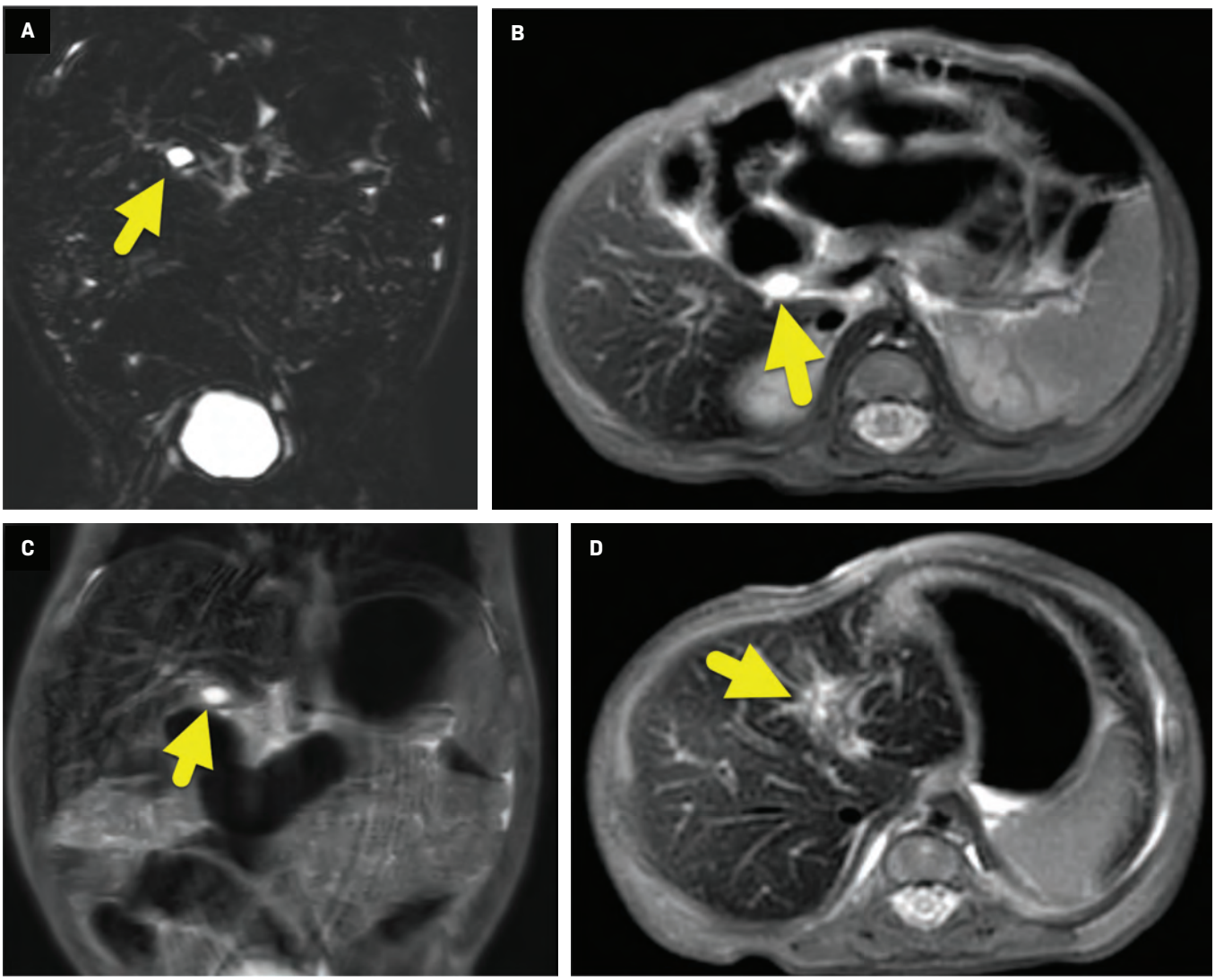

to peel from the inner cyst surface. There is also focal myofibroblastic hyperplasia enclosing the inner scarred layer.[7]

BA is treated via the Kasai procedure, which includes hepatic portoenterostomy, biliary remnant resection, and creation of Roux-en-Y intestinal anastomosis for bile flow.[1,6] If the Kasai procedure fails or the patient develops cirrhosis, a liver transplant is required.[6] Treatment after 60 postnatal days can accelerate hepatic fibrosis and liver failure, worsening patient outcomes.[2,6] The rapid development of cirrhosis in patients with BA makes it crucial to differentiate CBA from choledochal cyst.

CBA and choledochal cyst have many clinical and imaging similarities, which can make distinguishing between CBA and choledochal cyst challenging. Gallbladder morphology, triangular cord thickness, and cyst size, contents, and progression are used to differentiate CBA from choledochal cyst. A normal-sized gallbladder (> 15 mm) is characteristic of choledochal cyst, whereas an atretic (< 15 mm) or abnormally shaped (tubular or elongated) gallbladder is characteristic of CBA.[1,2,4] The triangular cord sign on US or MRI and a cyst size under 1.5 cm on prenatal US are diagnostic for CBA.[1,2,4] Prior studies have also demonstrated that the cyst size in CBA stays stable in the prenatal phase and regresses after birth. Patients with choledochal cyst had continuous growth of cysts

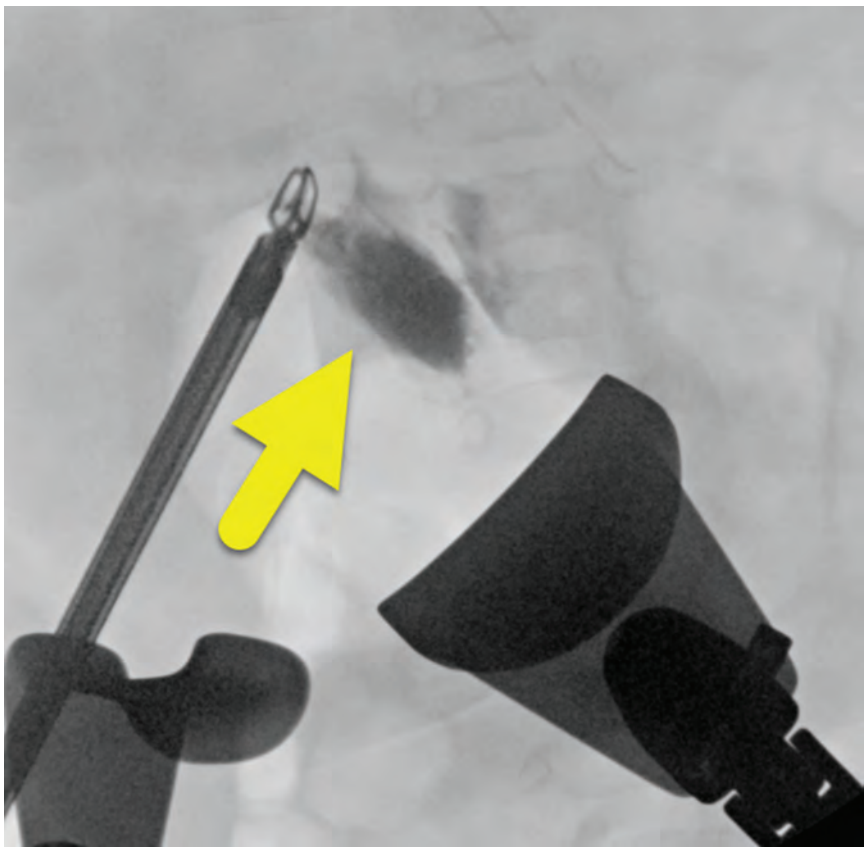

Figure 3. Intraoperative cholangiogram showed contrast injected directly into the cystic structure (arrow). There was no extension of contrast proximally into intrahepatic bile ducts or distally to the duodenum.

after birth.[4] When incised, choledochal cysts contain dark-green bile and biliary sludge, whereas cysts in patients with CBA have no content or small amounts of yellow fluid.[1,2,4]

Conclusion

CBA is an uncommon variant of BA. Distinguishing CBA from choledochal cyst is paramount for patients to receive timely treatment and have the best outcomes.

References

1) Schooler GR, Mavis A. Cystic biliary atresia: a distinct clinical entity that may mimic choledochal cyst. *Radiol Case Rep*. 2018;13(2):415-418. doi:10.1016/j.radcr.2018.01.025

2) Shin HJ, Yoon H, Han SJ, et al. Key imaging features for differentiating cystic biliary atresia from choledochal cyst: prenatal ultrasonography and postnatal ultrasonography and MRI. *Ultrasonography*. 2021;40(2):301-311. doi:10.14366/usg.20061

3) Hartley JL, Davenport M, Kelly DA. Biliary atresia. *Lancet*. 2009;374(9702):1704-1713. doi:10.1016/S0140-6736(09)60946-6

4) Chen Y-T, Gao M-J, Zheng Z-B, et al. Comparative analysis of cystic biliary atresia and choledochal cysts. *Front Pediatr*. 2022;10:947876. doi:10.3389/fped.2022.947876

5) Brahee DD, Lampl BS. Neonatal diagnosis of biliary atresia: a practical review and update. *Pediatr Radiol*. 2022;52(4):685-692. doi:10.1007/s00247-021-05148-y

6) Vij M, Rela M. Biliary atresia: pathology, etiology, and pathogenesis. *Future Sci OA*. 2020;6(5):FSO466. doi:10.2144/fsoa-2019-0153

7) Lobeck IN, Sheridan R, Lovell M, et al. Cystic biliary atresia and choledochal cysts are distinct histopathologic entities. *Am J Surg Pathol*. 2017;41(3):354-364. doi:10.1097/PAS.0000000000000805

Recurrent Respiratory Papillomatosis

Dalia Koujah; Richard B. Towbin, MD; Carrie M. Schaefer, MD; Alexander J. Towbin, MD

Case Summary

An adolescent with a history of recurrent respiratory papillomatosis (RRP) and pulmonary involvement presented with progressive dyspnea on exertion.

Imaging Findings

Chest radiograph (Figure 1) and chest CT (Figure 2) showed both cystic and solid lesions. The cystic lesions had a variable appearance: Some had a thick, irregular wall while others had a thin, nearly imperceptible wall. A small nodule was visible in the posterolateral trachea on CT.

Diagnosis

Recurrent respiratory papillomatosis

Discussion

Recurrent respiratory papillomatosis is a rare disease characterized by recurrent benign papillomas that can occur anywhere along the respiratory tract, most commonly the larynx and vocal cords. Globally, the incidence of RRP is 4 per 100,000 children and 2 per 100,000 adults.[1] Rates in the US have been steadily declining since the introduction of the human papillomavirus (HPV) vaccine in 2006.[2] The current estimated incidence of RRP in children is 4 per 100,000 children and 2 per 100,000 in adults annually.[3]

Specific types of HPV, most commonly HPV 6 and HPV 11, are associated with the wart-like papilloma characteristic of RRP.[3] HPV 11 is associated with more aggressive disease, often seen in children less than 5 years old.[4]

Recurrent respiratory papillomatosis has a trimodal age distribution, with age peaks at 7, 35, and 64 years,[3] and is classified as juvenile- or adult-onset. Patients with juvenile-onset RRP present between 2 and 6 years old with more aggressive disease[5] transmitted vertically either in utero or during passage through an infected birth canal. The etiology of adult-onset RRP is unclear, with some sources favoring transmition via oral-genital contact while others favor genetic susceptibility, including adult activation of vertically transmitted disease.[6,7,8] Upon infection, the virus remains latent within the host cells, causing recurrences even after the elimination of the initial papilloma.

Papillomas are found primarily in the larynx, although they can occur anywhere in the airway, from the nasopharynx to the tracheobronchial tree and pulmonary parenchyma. Clinical presentation is nonspecific and dependent on the location of the lesions. Potential signs include voice changes, cough, dyspnea, wheezing, and stridor. In adults, hoarseness is the most common presenting sign. In children, presenting signs include progressive hoarseness, stridor, and breathing difficulties.[5] Owing to the nonspecific signs, children are often treated for pharyngitis, asthma, or bronchitis, resulting in delayed diagnosis and potential for progression to respiratory distress.

Disease course is highly variable, ranging from spontaneous remission to malignant transformation. Squamous cell carcinoma resulting from RRP is rare but has a poor prognosis. Malignant transformation is more commonly associated with HPV 16 and 18, smoking, and radiation therapy.[9] Disease recurrence is associated with diminished lymphocyte response, although it remains unclear whether this is causative or a result of infection.[10]

Recurrent respiratory papillomatosis is rarely diagnosed via chest radiograph, although it can be visualized as solid or cavitated pulmonary nodules if there is lung involvement. In severe cases, chest radiograph may demonstrate symptoms of bronchial

Affiliations: University of Arizona College of Medicine, Phoenix Campus, Phoenix, Arizona (Koujah); Department of Radiology, Phoenix Children's Hospital, Phoenix, Arizona (RB Towbin, Schaefer); Department of Radiology, Cincinnati Children's Hospital, University of Cincinnati College of Medicine, Cincinnati, Ohio (AJ Towbin).

Published: October 1, 2024. https://doi.org/10.1016/10.37549/AR-D-24-0019

Figure 1. Chest radiograph shows multiple cystic (solid arrows) and solid (dashed arrow) lesions in the lungs.

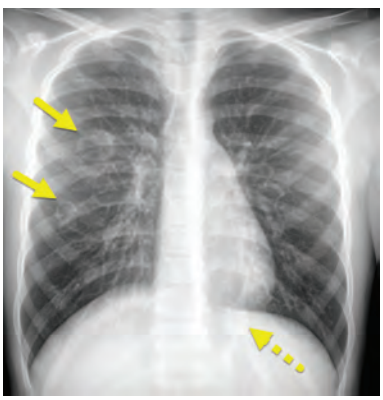

obstruction such as atelectasis and bronchiectasis.[4]

CT is the preferred imaging modality and can demonstrate the tracheal and bronchial lesions characteristic of RRP. Nodular lesions can present on CT as focal or diffuse large airway narrowing. Lung lesions may be single or multiple, nodular or polypoid, and of varying size and distribution.[4] In some cases, lesions can present as enlarged air-filled cysts, and superimposed infection can cause air-fluid levels. CT findings of airway obstruction include atelectasis and bronchiectasis.[11]

Diagnosis is confirmed via laryngoscopy and bronchoscopy, allowing direct visualization of the vocal cords and airways, as well as biopsy for histopathological examination. Papillomas are often visualized as pale polypoid lesions along the respiratory tract. Definitive diagnosis is made via histopathological examination, which shows well-differentiated squamous epithelium with a central fibrovascular core.[12]

Figure 2. Chest CT through the trachea (A), subcarinal region (B), pulmonary vein insertion (C), and lung bases (D) shows multiple lesions in the airways. Some cystic lesions have a thick, irregular wall (arrows) while others have a barely perceptible wall (yellow arrowhead). Solid pulmonary nodules are also present (dashed arrows). A papilloma (orange arrowhead) is visible along the left posterolateral aspect of the trachea.

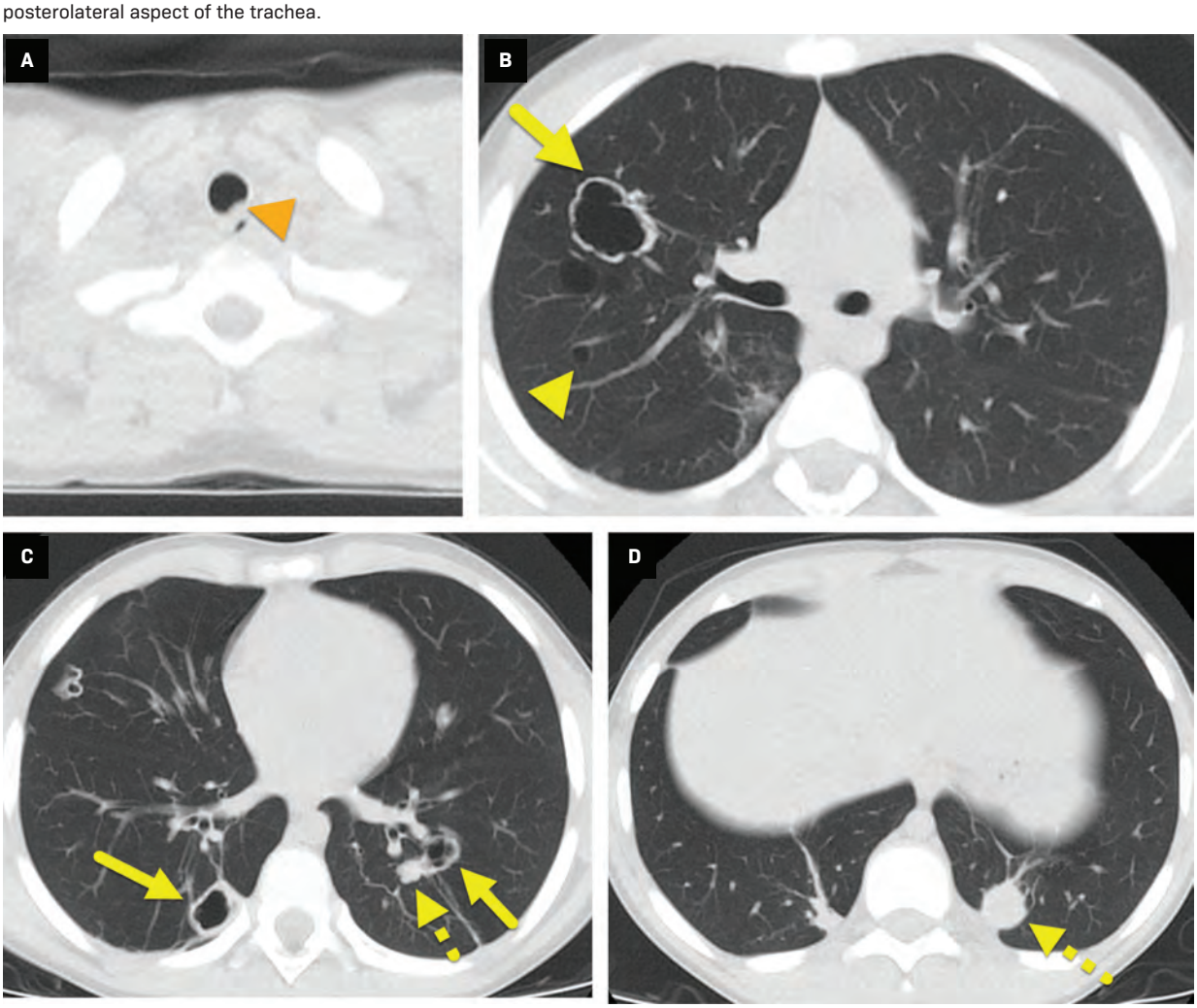

Currently there is no cure for RPP. Papillomas are primarily treated surgically, with adjunct therapy recommended in approximately 20% of patients.[4] Clinical criteria for adjunct therapy include greater than 4 surgical procedures per year, rapid regrowth with airway obstruction, or distal multisite spread.[13] Adjunct therapy includes antiviral medications, COX-2 inhibitors, and chemotherapeutics.

Conclusion

Recurrent respiratory papillomatosis is a rare disorder of benign neoplasms of the respiratory tract, commonly located along the larynx and vocal cords. It is most commonly associated with HPV 6 and HPV 11 infection, and has a trimodal age distribution, with more aggressive disease in children. If left untreated, RRP can lead to significant respiratory distress and may lead to the development of squamous cell carcinoma. Although there is no cure, surgical excision improves symptoms. The HPV vaccine has helped decrease the incidence of RRP.

References

1) Derkay CS, Wiatrak B. Recurrent respiratory papillomatosis: a review. *Laryngoscope*. 2008;118(7):1236-1247. doi:10.1097/MLG.0b013e31816a7135

2) Meites E, Stone L, Amiling R, et al. Significant declines in juvenile-onset recurrent respiratory papillomatosis following human papillomavirus (HPV) vaccine introduction in the United States. *Clin Infect Dis*. 2021;73(5):885-890. doi:10.1093/cid/ciab171

3) Sechi I, Muresu N, DiLorenzo B, et al. Pulmonary involvement in recurrent respiratory papillomatosis: a systematic review. *Infect Dis Rep*. 2024;16(2):200-215. doi:10.3390/idr16020016

4) Fortes HR, von Ranke FM, Escuissato DL, et al. Recurrent respiratory papillomatosis: a state-of-the-art review. *Respir Med*. 2017;126:116-121. doi:10.1016/j.rmed.2017.03.030

5) Benedict JJ, Derkay CS. Recurrent respiratory papillomatosis: a 2020 perspective. *Laryngoscope Investig Otolaryngol*. 2021;6(2):340-345. doi:10.1002/lio2.545

6) Gerein V, Schmandt S, Babkina N, et al. Human papilloma virus (HPV)-associated gynecological alteration in mothers of children with recurrent respiratory papillomatosis during long-term observation. *Cancer Detect Prev*. 2007;31(4):276-281. doi:10.1016/j.cdp.2007.07.004

7) Sabry AO, Papilloma PBC. Papilloma. [updated 2023 aug 14]. *StatPearls [Internet]*. StatPearls Publishing. 2024. https://www.ncbi.nlm.nih.gov/books/NBK560737/

8) Carifi M, Napolitano D, Morandi M, Dall'Olio D. Recurrent respiratory papillomatosis: current and future perspectives. *Ther Clin Risk Manag*. 2015;11:731-738. doi:10.2147/TCRM.S81825

9) Katsenos S, Becker HD. Recurrent respiratory papillomatosis: a rare chronic disease, difficult to treat, with potential to lung cancer transformation: apropos of two cases and a brief literature review. *Case Rep Oncol*. 2011;4(1):162-171. doi:10.1159/000327094

10) Stern Y, Felipovich A, Cotton RT, Segal K. Immunocompetency in children with recurrent respiratory papillomatosis: prospective study. *Ann Otol Rhinol Laryngol*. 2007;116(3):169-171. doi:10.1177/000348940711600302

11) Pai SI, Wasserman I, Ji YD, et al. Pulmonary manifestations of chronic HPV infection in patients with recurrent respiratory papillomatosis. *Lancet Respir Med*. 2022;10(10):997-1008. doi:10.1016/S2213-2600(22)00008-X

12) Ko JM, Jung JI, Park SH, et al. Benign tumors of the tracheobronchial tree: CT-pathologic correlation. *AJR Am J Roentgenol*. 2006;186(5):1304-1313. doi:10.2214/AJR.04.1893

13) Torres-Canchala L, Cleves-Luna D, Arias-Valderrama O, et al. Systemic bevacizumab for recurrent respiratory papillomatosis: a scoping review from 2009 to 2022. *Children (Basel)*. 2022;10(1):54. doi:10.3390/children10010054

Klippel-Trenaunay Syndrome

Brenden C. Maag, BS; Richard B. Towbin, MD; Carrie M. Schaefer, MD; Alexander J. Towbin, MD

Case Summary

An infant presented with a large port-wine stain of the right lower extremity, pelvis, and trunk that was present at birth. Additionally, the right lower extremity was larger than the left and there was intermittent bleeding from skin lesions of the right lower extremity. A punch biopsy of a skin lesion was performed for genetic testing, documenting a somatic, pathogenic PIK3CA variant. The diagnosis was PIK3CA-related overgrowth spectrum, and the phenotype was consistent with Klippel-Trenaunay syndrome (KTS).

Imaging Findings

MRI of the lower extremities and pelvis showed the abnormalities (Figure 1), including a large lateral marginal vein extending from the foot to the proximal thigh, which drains centrally. Additionally, there were scattered lymphatic and venous malformations in the right lower extremity.

Affiliations: University of Central Florida College of Medicine, Orlando, Florida (Maag); Department of Radiology, Phoenix Children's Hospital, Phoenix, Arizona (RB Towbin, Schaefer); Department of Radiology, Cincinnati Children's Hospital, University of Cincinnati College of Medicine, Cincinnati, Ohio (AJ Towbin).

Diagnosis

Klippel-Trenauney syndrome (KTS)

Differential Diagnosis

CLOVES Syndrome

The limb overgrowth and port wine stains seen in KTS manifest similarly to CLOVES (congenital lipomatous overgrowth, vascular malformations, epidermal nevi, and scoliosis/skeletal/spinal/anomalies) syndrome, another manifestation of PIK3CA gene mutations. In CLOVES, truncal involvement with vascular malformations and fatty overgrowth is more common. Additionally, tethered spinal cord, scoliosis, and renal abnormalities such as Wilms tumor are associated with CLOVES syndrome but are not typically seen in KTS.

Proteus Syndrome

Proteus syndrome results from a mutation in the AKT1 gene pathway, resulting in an asymmetric overgrowth pattern that can affect all body parts. When unilateral, this may appear similarly to the overgrowth seen in KTS, but Proteus syndrome presents much more frequently with progressive skeletal abnormalities and pulmonary disease.

Maffucci Syndrome

Maffucci syndrome is due to an IDH1 gene mutation and initially presents with enchondromas in the long bones of the arms and legs. Vascular malformations associated with this syndrome are progressive but usually present at 5 years of age or older. The primary risk of this syndrome is the development of chondrosarcoma.

Sturge-Weber Syndrome

Sturge-Weber syndrome is another genetic disorder that results from a mutation of the GNAQ gene and is associated with facial port-wine stains and vascular malformations, although the malformations are almost always seen in the brain. Additionally, these patients often have delays in cognitive development and ophthalmologic abnormalities, which are not seen in isolated KTS.

Discussion

The diagnosis of KTS is usually clinical. The initial diagnostic imaging modality of choice is often Doppler US, which allows for visualization of the varicosities as well as appreciation of any concurrent thrombosis or venous insufficiency. The extent of the US findings directly relates to disease severity. Once extensive venous

Published: October 1, 2024. https://doi.org/10.1016/10.37549/AR-D-24-0014

Figure 1. MRI (A, B). Coronal STIR (A) and MR venography (B) of the lower extremities and pelvis. A large lateral marginal vein extends from the foot to the proximal thigh (blue arrow), where it continues as the sciatic vein (red asterisk) and then drains into the right internal iliac vein (green arrow). The lateral marginal and sciatic veins are persistent embryonic veins. The right lower-extremity deep veins are hypoplastic. Note the normal left femoral vein (black arrow). Additionally, scattered lymphatic and venous malformations are shown in the right lower extremity (yellow arrows).

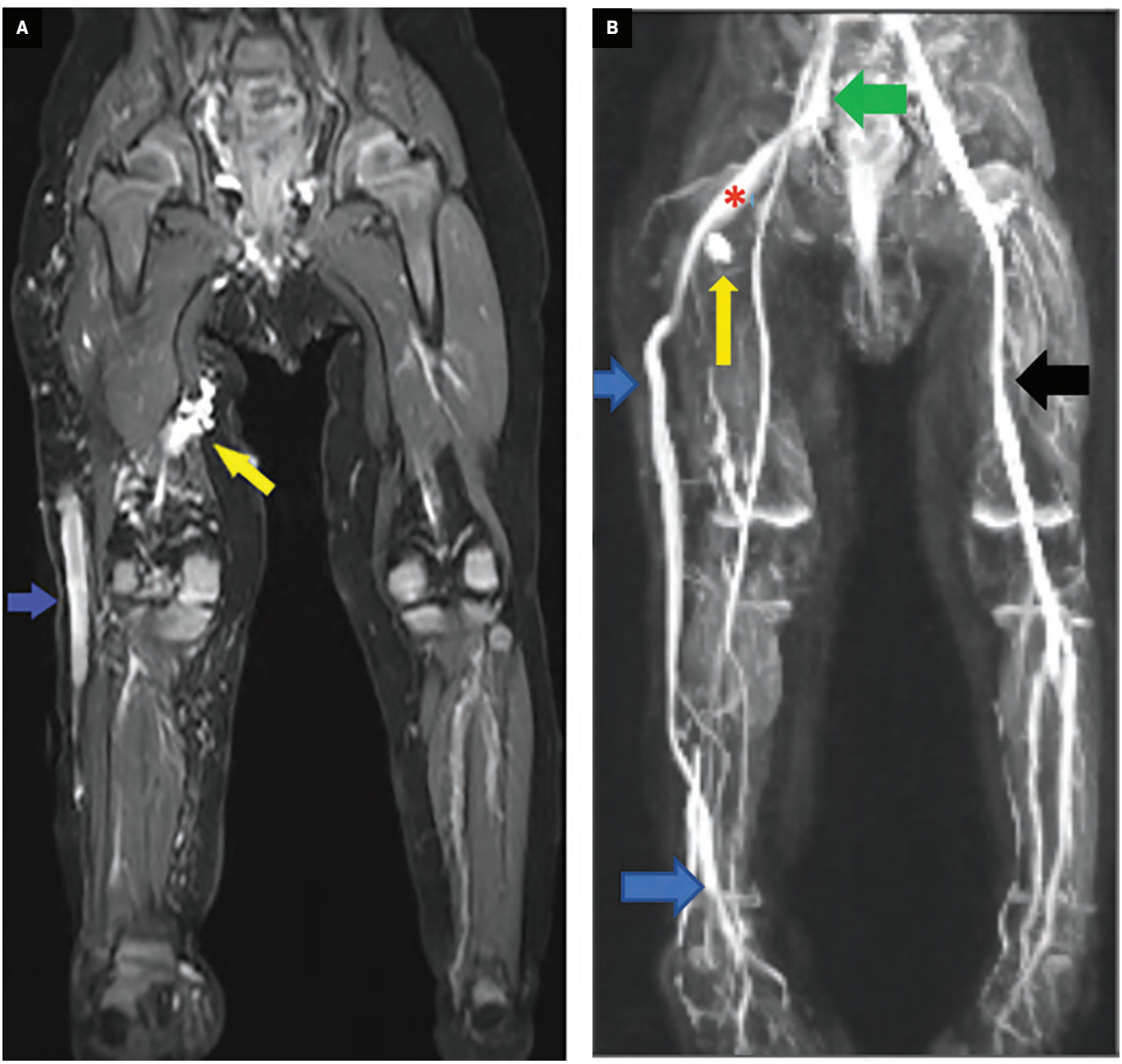

thrombosis is noted in the setting of possible KTS or a therapeutic intervention is considered, CT or MRI is often needed to determine disease extent. Additionally, these imaging modalities can evaluate for other malformations, including spinal cavernous malformations, pulmonary anomalies, and gastrointestinal malformations.[1]

KTS is an uncommon pediatric disease characterized by an activating mutation in the PIK3CA gene, resulting in global or focal tissue overgrowth. The disease is a common subtype of PIK3CA-related overgrowth syndromes and has a variable but classic presentation due to the mosaic pattern of gene mutation.[1] KTS is also associated

with a triad of cutaneous angiomas, venous and lymphatic abnormalities, and soft-tissue or bony hypertrophy. A diagnosis of KTS requires 2 of these 3 features.[2,3] These abnormalities have various clinical consequences, predominantly limb pain, fatigue, and recurrent superficial and deep-vein thrombosis.[4] On examination, children with KTS have overgrowth of the affected limbs and/or cutaneous malformations on the trunk. Port-wine stains are the most common skin finding, which are cutaneous manifestations of the underlying capillary malformations.

The focus of therapy in refractory KTS is obliteration or removal of the persistent embryonic veins, which are the common cause of signs and symptoms. The 2 vessels that constitute the most problematic veins in the leg are the lateral marginal vein (LMV) and the persistent sciatic vein (PSV).[5] The LMV is an embryonic vessel that originates on the dorsal side of the foot and eventually contributes to the small saphenous vein and superficial venous system before naturally regressing. The PSV is a deep vein of the posterior thigh considered the major tributary of the developing deep-venous system before regressing. When these vessels persist, they disrupt the physiological growth of normal venous anatomy and often dilate to large diameters, greatly increasing the risk of venous stasis. When severe, this can result in life-threatening complications, including large-volume bleeding, pulmonary emboli, and venous thromboses.[2] Despite being a common in affected children, the prevalence of these marginal veins is conservatively measured at around 15% to 20%, likely due to the highly variable phenotype of KTS.[5]

When these embryonic veins only cause mild and nondisruptive symptoms, conservative treatment with compression stockings, pain control, and avoidance of injury are the first-line treatment. Traditionally, surgery has been the primary treatment method for severe or refractory cases. The surgical approach depends on disease extent and usually includes vein stripping, stab phlebectomies (whereby the vein is hooked through a small excision, brought outside the skin, and removed), and gross excision.

Surgery has largely been replaced by more minimally invasive techniques, including embolization using coils, vascular plugs and other materials, endovenous laser ablation therapy (EVLT) such as radiofrequency ablation (RFA), and sclerotherapy. These methods occlude abnormal veins and avoid the potential surgical complications of poor wound closure and persistent bleeding, and are first-line therapies for persistent KTS.[1] Other ablative techniques, such as cryoablation, cannot currently deliver therapy to the entire embryonic vessel, which could result in collateralization and incomplete response. The best approach is not yet known.

EVLT can be used to treat persistent embryonic veins, and acts by emitting a wavelength of light that generates photon-induced damage to the vessel wall as well as thermal damage to the surrounding area.[6] EVLT is generally well-tolerated, with complications including ecchymosis, skin burns, and thrombophlebitis along the ablated vein. Rarely, heat-induced thrombus may occur, which is defined as postprocedural thrombus propagating into deeper vessels cephalad to the treated area.[7] RFA may cause tissue necrosis in a localized area by agitating adjacent molecules and producing high temperatures.[7] The complications of RFA are the same as those of EVLT, owing to the similar method of heat-induced vascular damage.[8]

Sclerotherapy can treat a variety of vascular diseases, including the persistent embryonic veins in KTS.[9] In sclerotherapy, catheter injection of a sclerosant, either alone or in combination with other minimally invasive techniques, damages the intimal wall of the vessel and induces thrombosis. A variety of agents can be used based on radiologist preference. Modern agents include polidocanol and sodium tetradecyl sulfate, which thrombose the target vessel while avoiding the local destruction and ischemia that can occur with the high doses of ethanol needed to treat large vessels.[10] Complications of sclerotherapy, such as deep-vein thrombosis and extension of thrombosis past the target lesion into a deeper venous system, can occur. More severe complications can result in both transient and permanent neurological deficits, including visual disturbance, migraine, stroke, and, rarely, death.[6] The expected rate of neurological disturbance is less than 2%, with permanent damage even more rare.[6]

Conclusion

KTS is a disease that, when severe, has devastating clinical consequences, including severe bleeding, deep-vein thrombosis, and pulmonary emboli. Although the presentation of KTS is variable, the classic triad is cutaneous angiomas, venous and lymphatic abnormalities, and tissue overgrowth.. When KTS is suspected in a child with unilateral extremity overgrowth, imaging will help identify the problematic embryonic vein(s), both the LMV and the PSV. US will demonstrate a persistently dilated embryonic vein with thrombosis, and MRI can determine the extent of the lesion.

MRI will additionally characterize the soft tissue and bony overgrowth and allow for treatment planning. Treatment for this syndrome has historically been surgical, which can be associated with significant complications. New minimally invasive techniques, including RFA, EVLT, and sclerotherapy, have expanded treatment options with fewer complications.

References

1) Martinez-Lopez A, Blasco-Morente G, Perez-Lopez I, et al. CLOVES syndrome: review of a PIK3CA-related overgrowth spectrum (PROS). *Clin Genet*. 2017;91(1):14-21. doi:10.1111/cge.12832

2) John PR. Klippel-Trenaunay syndrome. *Tech Vasc Interv Radiol*. 2019;22(4):100634. doi:10.1016/j.tvir.2019.100634

3) Berry SA, Peterson C, Mize W, et al. Klippel-Trenaunay syndrome. *Am J Med Genet*. 1998;79(4):319-326.

4) Anderson KR, Nguyen H, Schoch JJ, et al. Skin-related complications of Klippel-Trenaunay syndrome: a retrospective review of 410 patients. *J Eur Acad Dermatol Venereol*. 2021;35(2):517-522. doi:10.1111/jdv.16999

5) Oduber CEU, Young-Afat DA, van der Wal AC, et al. The persistent embryonic vein in Klippel-Trenaunay syndrome. *Vasc Med*. 2013;18(4):185-191. doi:10.1177/1358863X13498463

6) Gillet JL, Guedes JM, Guex JJ, et al. Side-effects and complications of foam sclerotherapy of the great and small saphenous veins: a controlled multicentre prospective study including 1,025 patients. *Phlebology*. 2009;24(3):131-138. doi:10.1258/phleb.2008.008063

7) Schmedt CG, Sroka R, Steckmeier S, et al. Investigation on radiofrequency and laser (980 nm) effects after endoluminal treatment of saphenous vein insufficiency in an ex-vivo model. *Eur J Vasc Endovasc Surg*. 2006;32(3):318-325. doi:10.1016/j.ejvs.2006.04.013

8) Hong K, Georgiades C. Radiofrequency ablation: mechanism of action and devices. *J Vasc Interv Radiol*. 2010;21(8 suppl):S179-86. doi:10.1016/j.jvir.2010.04.008

9) Blaise S, Charavin-Cocuzza M, Riom H, et al. Treatment of low-flow vascular malformations by ultrasound-guided sclerotherapy with polidocanol foam: 24 cases and literature review. *Eur J Vasc Endovasc Surg*. 2011;41(3):412-417. doi:10.1016/j.ejvs.2010.10.009

10) Willenberg T, Smith PC, Shepherd A, Davies AH. Visual disturbance following sclerotherapy for varicose veins, reticular veins and telangiectasias: a systematic literature review. *Phlebology*. 2013;28(3):123-131. doi:10.1258/phleb.2012.012051

Orbital Rhabdoid Tumor

Joshua V. Valbuena, BS; Richard B. Towbin, MD; Daniel Morgan, DO; Carrie M. Schaefer, MD; Alexander J. Towbin, MD

Case Summary

An infant presented with a 2-week history of a bulging left eye, with proptosis and entrapment. Orbital CT and MRI revealed a left orbital mass. Biopsy revealed that the mass was a rhabdoid tumor (RT), and the patient subsequently underwent chemotherapy. Treatment significantly decreased the mass.

Imaging Findings

Orbital CT with contrast (Figure 1) and orbital MRI without and with contrast (Figure 2) revealed a heterogeneously enhancing 3.6 × 1.7-cm retrobulbar mass in the left orbit. No intracranial extension was noted. CT of the chest, abdomen, and pelvis showed no metastatic disease.

Diagnosis

Rhabdoid tumor.

The differential diagnosis includes other similar round-cell tumors such as neuroblastoma and rhabdomyosarcoma.

Discussion

RT of the orbit was initially described as a sarcomatous variant of Wilms tumor in 1978. However, since then it has been recognized as a distinct entity.[1] RTs have a wide phenotypic range and can be present in many parts of the body. According to a population study using data from the Surveillance, Epidemiology, and End Results (SEER) program, RTs most commonly arise in the central nervous system (CNS) (35%) and kidneys (20%), with the remaining 45% located extracranially.[2,3] An RT can occur anywhere in the brain or spine. CNS RT, also called atypical teratoid rhabdoid tumor, most commonly arises within the posterior fossa.[4-6]

Histologically, RTs have polygonal cells with eccentric nuclei and hyperchromatic nucleoli with vimentin and epithelial membrane antigen positivity.[2,7,8] Additionally, RTs are united by a loss-of-function mutation in the *SMARCB1* or, less commonly, *SMARCA4* tumor suppressor gene.[8] The presence of a mutation is diagnostic of MRT in the context

Figure 1. Axial contrast-enhanced CT shows a mildly enhancing mass (arrow) of the left orbit causing proptosis.

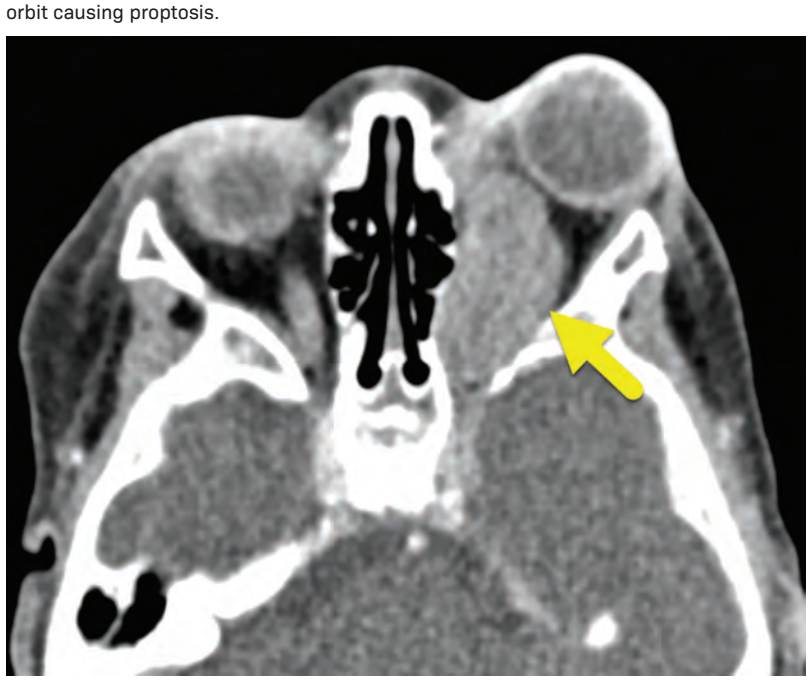

Affiliations: University of Arizona College of Medicine, Phoenix, Arizona (Valbuena); Department of Radiology, Phoenix Children's Hospital, Phoenix, Arizona (RB Towbin, Schaefer); University of Cincinnati College of Medicine, Cincinnati, Ohio (Morgan, AJ Towbin); Children's Hospital Medical Center, Cincinnati, Ohio (AJ Towbin).

Published: October 1, 2024. https://doi.org/10.1016/10.37549/AR-D-24-0017

Figure 2. Axial T1-weighted MRI (A) shows an isointense orbital mass (arrow) causing proptosis. Axial T2-weighted MRI (B) shows the lobulated mass (arrow) to be heterogeneous and mostly hypointense with small hyperintense foci. T1-weighted postcontrast MRI (C) showing the mass (arrow) to have mild peripheral enhancement.

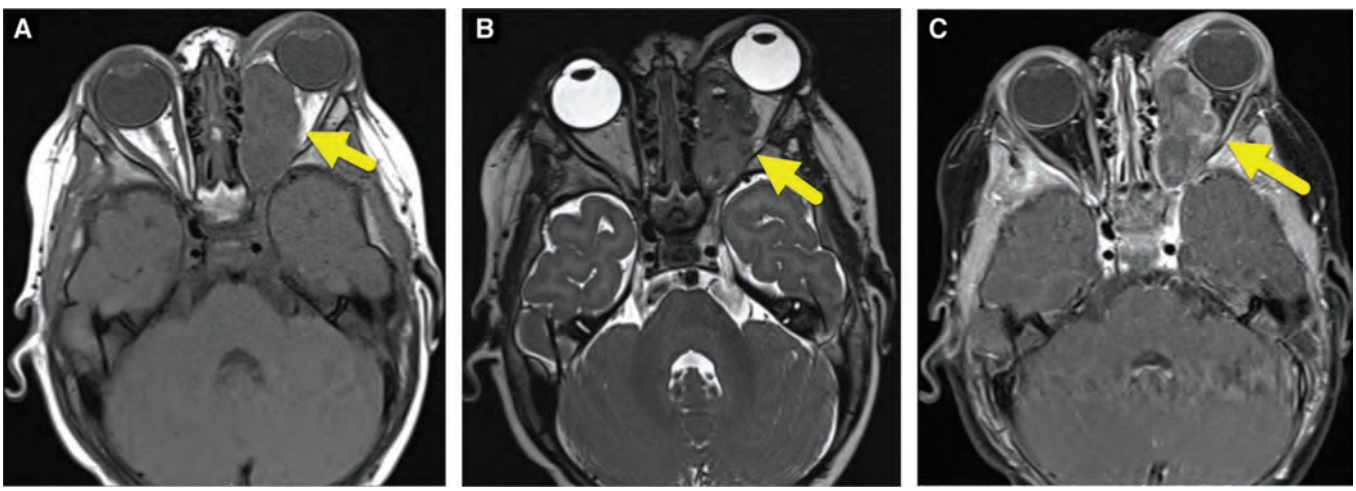

of poorly differentiated malignant rhabdoid cells.[8]

Orbital RTs are rare and typically occur in infants, with a mean age of diagnosis of 10.37 months ± 14.5 months. The tumors account for less than 1% of all RTs and occur in less than 1 in a million people. Diagnosis is most often made in children 11 to 18 months old.[3,7] Patients present with rapidly progressing proptosis, preauricular/submandibular lymphadenopathy, eyelid swelling, and loss of light reaction in the eye in more advanced cases.[7-9] Orbital RTs are not always confined to the orbit. CNS involvement has been linked with worse outcomes and poses a problem for the possibility of resection.[10] Unfortunately, orbital RTs have a poor prognosis, with a 3-year survival rate of 9%.[6]

MRI is the most useful modality to assess the disease extent owing to its ability to assess intracranial extension and optic nerve involvement. CT is helpful when an MRI cannot be obtained or when bone destruction is suspected. Orbital RT appears as a heterogeneous retrobulbar, intraconal mass causing proptosis on MRI. It is hypo- to isointense on T1-weighted images, iso- to hyperintense on T2-weighted images with areas of edema, calcification, and hemorrhage, and inhomogeneously enhances after the administration of gadolinium-based contrast media. If CT is performed, the mass appears as a heterogeneous, hypodense solid mass. The tumor does not typically enhance after the administration of iodinated contrast media. CT of the chest and CT or MRI of the abdomen and pelvis are frequently performed to assess the presence of metastatic disease.

Treatment guidelines are not well established for this rare disease, but multimodal approaches have been used with some success in decreasing tumor burden. These approaches include combination chemotherapy, radiotherapy, and/or stereotactic radiosurgery.[9] Most tumors are ultimately resected and the globe enucleated.

Conclusion

Orbital RT is a rare tumor that presents with rapid progression of proptosis and eye swelling. The tumor is typically characterized via imaging with CT and MRI and diagnosed via biopsy. Patients are treated with a multimodal approach. Orbital RTs have a poor prognosis, and continued improvements in therapy are needed.

References

1) Beckwith JB, Palmer NF. Histopathology and prognosis of Wilms tumors: results from the first national Wilms' tumor study. *Cancer*. 1978;41(5):1937-1948. doi: 10.1002/1097-0142(197805)41:5<1937::AID-CNCR2820410538>3.0.CO;2-U

2) Rootman J, Damji KF, Dimmick JE. Malignant rhabdoid tumor of the orbit. *Ophthalmology*. 1989;96(11):1650-1654. doi:10.1016/s0161-6420(89)32666-2

3) Sultan I, Qaddoumi I, Rodríguez-Galindo C, et al. Age, stage, and radiotherapy, but not primary tumor site, affects the outcome of patients with malignant rhabdoid tumors. *Pediatr Blood Cancer*. 2010;54(1):35-40. doi:10.1002/pbc.22285

4) Dho Y-S, Kim S-K, Cheon J-E, et al. Investigation of the location of atypical teratoid/rhabdoid tumor. *Childs Nerv Syst*. 2015;31(8):1305-1311. doi:10.1007/s00381-015-2739-x

5) Gaillard F, Kumar K, Weerakkody Y, et al. Atypical teratoid/rhabdoid tumor. Reference article. Gaillard F. Atypical teratoid/rhabdoid tumor | Radiology Reference Article | Radiopaedia.org.Radiopaedia. doi:10.53347/rID-5897

6) Devnani B, Biswas A, Bakhshi S, Kaushal S, Nakra T. Extrarenal extracranial rhabdoid tumor of the pelvis in a young adult-management of a challenging case. *Indian J Med Paediatr Oncol*. 2017;38(3):383-386. doi:10.4103/ijmpo.ijmpo_108_17

7) Hada M, Chawla B, Seth R, Khurana S, Kashyap S. Primary intraocular malignant rhabdoid tumor presenting as orbital mass with intracranial extension in an adolescent. *Can J Ophthalmol*. 2017;52(1):e3-e5. doi:10.1016/j.jcjo.2016.07.023

8) Biswas A, Kumar R, Bakhshi S, Sen S, Sharma MC. Multimodal management of congenital orbital malignant rhabdoid tumor: review of literature and report of a rare case. *J Pediatr Hematol Oncol*. 2020;42(3):228-233. doi:10.1097/MPH.0000000000001402

9) Kook KH, Park MS, Yim H, et al. A case of congenital orbital malignant rhabdoid tumor: systemic metastasis following exenteration. *Ophthalmologica*. 2009;223(4):274-278. doi:10.1159/000213643

10) Watanabe H, Watanabe T, Kaneko M, et al. Treatment of unresectable malignant rhabdoid tumor of the orbit with tandem high-dose chemotherapy and Gamma-Knife radiosurgery. *Pediatr Blood Cancer*. 2006;47(6):846-850. doi:10.1002/pbc.20699

Pancreatic Divisum in Children

Nick Groth, BS; Richard B. Towbin, MD; Carrie M. Schaefer, MD; Alexander J. Towbin, MD

Case Summary

A teenager presented with chronic abdominal pain and severe nausea. The patient previously underwent surgery for median arcuate ligament syndrome, with persistent chronic abdominal pain, nausea, and vomiting as well as and progressive weight loss. One month prior to presentation, the patient was diagnosed with pancreatitis and dilated intra- and extrahepatic bile ducts with a common bile duct (CBD) stone on magnetic resonance cholangiopancreatography (MRCP). Additionally, pancreas divisum was noted on the MRCP.

Diagnosis

Pancreatic divisum (PD).

The differential diagnosis for PD includes gallstones, microlithiasis, medication-induced pancreatitis, autoimmune metabolic disorders, and other anomalies such as annular pancreas.[1]

Imaging Findings

Coronal MRCP sequence images (Figure 1A-C) show that the ventral (Wirsung) duct joins the CBD and drains into the duodenum via the major papilla. There is dilatation of the intra- and extrahepatic bile ducts as well as a stricture of the CBD. The distal dorsal pancreatic duct (Santorini) is shown emptying into the duodenum via the minor papilla, dorsal pancreatic duct. PD is diagnosed when the ducts of Wirsung and Santorini fail to fuse.

Discussion

PD is a congenital malformation of the pancreatic ducts, with a reported prevalence of approximately 10% in the general population. The anomaly is usually identified at autopsy with MRCP or with endoscopic retrograde cholangiopancreatography (ERCP) studies.[2] The clinical significance of PD has not been clearly defined, with more than 95% of these patients found to have PD incidentally, lacking pancreatic symptoms.[3] However, in the INSPPIRE (INternational Study Group of Pediatric Pancreatitis) cohort of children with acute recurrent or chronic pancreatitis, 14.6% were found to have PD, which is more than the general population.[4]

The embryological development of the pancreas starts around the fifth week when the pancreas starts as ventral and dorsal pancreatic buds. The ventral pancreatic bud originates in the hepatobiliary system, rotates, and fuses with the dorsal pancreatic bud originating in the foregut. The ventral bud contains the duct of Wirsung, and the dorsal bud, the duct of Santorini. As the CBD rotates, the 2 components fuse to form the main pancreatic duct of Wirsung, opening into the major papilla in the CBD. An accessory duct of Santorini from the dorsal bud can either atrophy or persist as an accessory duct.[5]

PD arises when the 2 ducts fail to fuse. The degree of this failure can result in several subtypes: (1) In classic PD (major variant), there is no communication between the 2 ducts; the ventral duct opens into the major papilla and the longer dorsal duct opens into the minor papilla. (2) When there is incomplete PD (minor variant), the anatomy is similar to the classic PD but with a small communication between the 2 ducts. (3) In reverse PD (rare variant), the duct of Santorini does not communicate with the main duct or the minor papilla.[3]

Due to most patients with PD being asymptomatic in the absence of additional risk factors such as cholelithiasis, cystic fibrosis, medications (most notably valproic acid and asparaginase), or mutations in genes encoding pancreatic enzymes, screening asymptomatic children is not recommended except for children with cystic fibrosis identified with an abnormal sweat chloride test.[1] Young children with pancreatitis, especially infants and toddlers, present with generalized abdominal pain and irritability

Affiliations: University of Arizona College of Medicine Phoenix Campus, Phoenix, AZ (Groth); Department of Radiology, Phoenix Children's Hospital, Phoenix, AZ (RB Towbin, Schaefer); Children's Hospital Medical Center, Cincinnati, OH (AJ Towbin); University of Cincinnati College of Medicine, Cincinnati, OH (AJ Towbin).

Published: October 1, 2024. https://doi.org/10.1016/10.37549/AR-D-24-0015

Figure 1. Posterior to anterior images. All images are a coronal MRCP sequence. The ventral (Wirsung) duct (A, yellow arrow) joins the CBD and drains into the duodenum via the major papilla. There is dilatation of the intra- and extrahepatic bile ducts as well as a stricture of the CBD (red arrow). The distal dorsal pancreatic duct (B, Santorini) empties into the duodenum via the minor papilla (blue arrow), dorsal pancreatic duct (C, blue arrows). Pancreatic divisum is diagnosed when the ducts of Wirsung and Santorini fail to fuse.

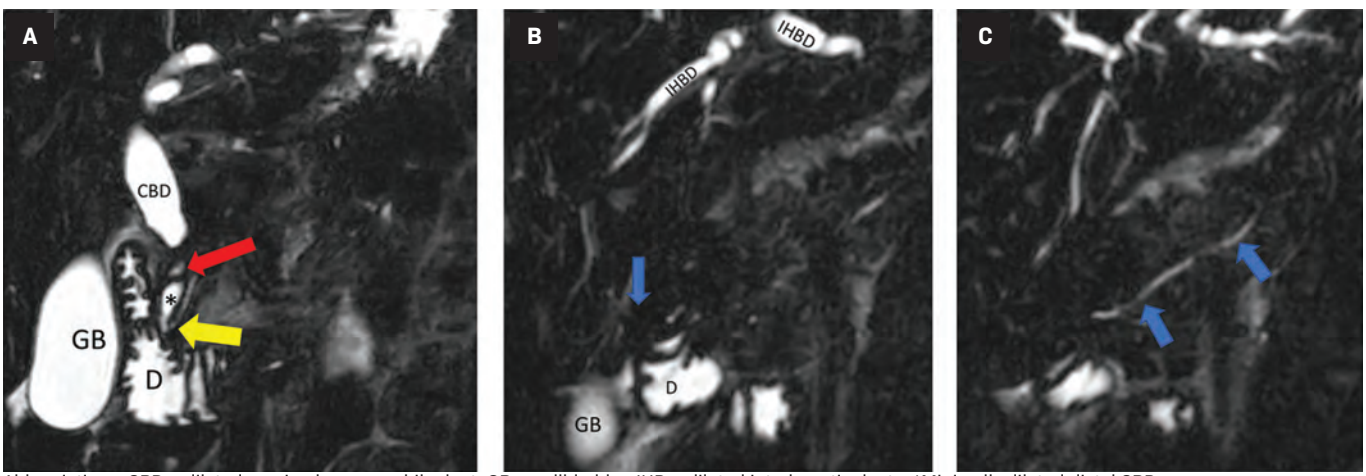

Abbreviations: CBD = dilated proximal common bile duct, GB = gallbladder, IHD = dilated intrahepatic ducts. *Minimally dilated distal CBD.

whereas adolescents and adults present with severe epigastric pain radiating to the back.[1] According to the INSPPIRE criteria, a diagnosis of acute pancreatitis in pediatric patients must meet 2 of 3 criteria: (1) abdominal pain, (2) serum lipase or serum amylase level 3 times the normal level, and (3) characteristic findings of acute pancreatitis on imaging.[6,7] Of note, serum lipase is a more reliable laboratory marker since amylase production is physiologically low in infants.[1]

Patients with asymptomatic PD require no further workup and treatment. Those with minor or infrequent symptoms are treated conservatively with a low-fat diet, analgesics, anticholinergics and, if necessary, pancreatic enzyme supplementation. Children with recurrent or severe symptoms warrant MRCP for evaluation and possible treatment of a stenotic minor papilla orifice or obstructive causes. Treatment of PD can include an endoscopic sphincterotomy, which is less invasive than a surgical sphincteroplasty.[3,7] Therapy should be based on morbidity, patient preference, and local institutional expertise.[3]

If a patient with PD presents with pancreatitis, oral feeding is recommended as soon as tolerated. If oral feeds are not tolerated or the required calories cannot be achieved in 72 hours, enteral tube feeding is recommended.[8] Aggressive fluid replacement therapy is recommended in children for the first 24 hours.[3] Analgesia should be provided when indicated, with an emphasis on nonopioid medications.[1,8] Endoscopic therapy for PD includes minor papilla endoscopic sphincterotomy, minor papilla orifice balloon dilation, and trans minor papilla duct stenting. Total pancreatectomy and islet auto transplantation is a surgical option to reduce the recurrence of chronic pancreatitis refractory to other therapies.[3,8]

Endoscopic US can diagnose PD, with a sensitivity of 87% to 95% with secretin enhancement to better visualize the ducts by stimulating pancreatic secretions.[3] Findings suggestive of pancreatic anomalies include the absence of the "stack sign" in which the distal CBD, ventral pancreatic duct, and portal vein run on a parallel axis in a normal pancreas. The presence of a "crossed duct sign," in which the dorsal pancreatic duct crosses over the bile duct anteriorly and superiorly, indicates the presence of PD.[3]

Contrast-enhanced abdominal CT is recommended only in pediatric patients who are clinically deteriorating. CT will visualize acute and chronic changes such as pancreatic atrophy and fat replacement but will not detect subtle parenchymal changes.[1] On contrast-enhanced CT, the findings are described as dorsal duct crossing anteriorly and superiorly to the distal CBD in the pancreatic head opening into minor papilla with a small ventral duct opening into the major papilla. CT sensitivity can be as low as 50% to 60% when there is pancreatic inflammation and is not desirable in childhood due to the radiation exposure.[1,3]

ERCP is considered the gold standard for diagnosing PD and can be used in this therapeutic setting but is not recommended for diagnostic purposes alone due to its invasive nature.[3,8] MRCP is comparable

to ERCP, and noninvasive MRCP is recommended for a suspected pancreatic ductal leak injury or suspected biliary tract abnormalities.[8] Sensitivity and specificity increase with secretin-enhanced MRCP to 83% to 86% and 97% to 99%, respectively. MRCP findings can include a Santorinicele, described as a cystic dilation of the dorsal duct near the opening of the minor papilla.[3] In addition to its lack of radiation exposure, MRCP is significantly more sensitive than CT for detecting chronic changes and irregularities of the pancreatic ducts and side branches.[1]

Conclusion

Although PD is a congenital malformation of the pancreas, pancreatitis is unlikely; however, there may be an increased risk. Imaging findings, including the crossed duct sign can diagnose PD. Patients should be treated for PD when they have associated severe or chronic pancreatitis.

References

1) Uc A, Husain SZ. Pancreatitis in children. *Gastroenterology*. 2019;156(7):1969-1978. doi:10.1053/j.gastro.2018.12.043

2) Bülow R, Simon P, Thiel R, et al. Anatomic variants of the pancreatic duct and their clinical relevance: an MR-guided study in the general population. *Eur Radiol*. 2014;24(12):3142-3149. doi:10.1007/s00330-014-3359-7

3) Gutta A, Fogel E, Sherman S. Identification, and management of pancreas divisum. *Expert Rev Gastroenterol Hepatol*. 2019;13(11):1089-1105. doi:10.1080/17474124.2019.1685871

4) Lin TK, Abu-El-Haija M, Nathan JD, et al. Pancreas divisum in pediatric acute recurrent and chronic pancreatitis: report from INSPPIRE. *J Clin Gastroenterol*. 2019;53(6):e232-e238. doi:10.1097/MCG.0000000000001063

5) Stern CD. A historical perspective on the discovery of the accessory duct of the pancreas, the ampulla "of Vater" and pancreas divisum. *Gut*. 1986;27(2):203-212. doi:10.1136/gut.27.2.203

6) Morinville VD, Husain SZ, Bai H, et al. Definitions of pediatric pancreatitis and survey of current clinical practices. *J Pediatr Gastroenterol Nutr*. 2012;55(3):261-265. doi:10.1097/MPG.0b013e31824f1516

7) Lehman GA, Sherman S, Nisi R, Hawes RH. Pancreas divisum: results of minor papilla sphincterotomy. *Gastrointest Endosc*. 1993;39(1):1-8. doi:10.1016/s0016-5107(93)70001-2

8) Párniczky A, Abu-El-Haija M, Husain S, et al. EPC/HPSG evidence-based guidelines for the management of pediatric pancreatitis. *Pancreatology*. 2018;18(2):146-160. doi:10.1016/j.pan.2018.01.001

Solid Pseudopapillary Tumor of the Pancreas

EA Sanchez Perez; Alexander J. Towbin, MD; Daniel Morgan, DO; Richard B. Towbin, MD

Case Summary

A teenager to the emergency room after a motor vehicle collision and 5 weeks following Caesarean-section. The chief complaint was of left lower-quadrant abdominal pain. Computed tomography showed no traumatic injury but identified a pancreatic tail mass. Subsequent laboratory testing revealed normal lipase and cancer antigen 19-9 levels.

Imaging Findings

Computed tomography imaging (Figure 1) showed an oval, well-circumscribed, 9.5-cm mass arising from the tail of the pancreas. The mass had a heterogeneous appearance with solid and cystic regions. It compressed the splenic vein, causing large splenic collateral vessels.

On MRI (Figure 2), the mass appeared heterogeneous, with layering hemorrhage on T2-weighted images. Postcontrast images showed mild enhancement of the irregular soft-tissue component. The areas of enhancement also displayed restricted diffusion.

Diagnosis

Solid pseudopapillary tumor (SPT) of the pancreas.

Differential diagnosis includes mucinous cystadenoma, mucinous cystadenocarcinoma, pancreatoblastoma, pancreatic adenocarcinoma, and pancreatic neuroendocrine tumor.

Discussion

An SPT of the pancreas is a low grade neoplasm of the exocrine parenchyma characterized by heterogeneous components of a cystic and/or solid nature.[1] The latter characteristic had given rise to various names commonly used in the literature.[2] Such names include solid and cystic acinar tumor, papillary epithelial neoplasm, solid pseudopapillary epithelial neoplasm, and Gruber-Frantz tumor.[1,3-6]

Solid psuedopapillary tumors of the pancreas have a relatively low incidence, accounting for 1% of pancreatic neoplasms, 6% of all exocrine subtypes, and 8 to 17% of pediatric pancreatic tumors, noting that pancreatic tumors are highly unusual in children.[3,5] This type of pancreatic neoplasm has a disproportionately high 1:5.3-10 male-to-female (M:F) ratio and typically occurs during the third decade of life.[2,5-8] Papavramidis et al showed that SPTs are more likely to be diagnosed in children.[5] In their study, 22% of patients were diagnosed when younger than 19 years of age while only 6% of patients were diagnosed when older than 51 years.[5]

The predilection for the tumor to occur in young women suggests that reproductive hormones, such as estrogen, may play a role in the pathogenesis of SPT of the pancreas. This theory is supported by data showing that postmenopausal women with SPT have a smaller tumor size compared with premenopausal women.[7] Also, pediatric series have reported M:F ratios between 1:1.75-6.5, lower than the ratio seen in adults.[8]

Incidental detection, as seen here, is relatively common. When symptomatic, patients typically present with vague abdominal pain, bloating, and discomfort.[2-69,,10] Other signs can include a palpable abdominal mass or more nonspecific presentations such asnausea, vomiting, and weight loss.[6] Tumors in the pancreatic head may eventually cause obstructionand signs associated with biliary backflow and obstruction (eg, jaundice, pancreatitis).[2-7]

Diagnosis is usually made using fine-needle aspiration (FNA)

Affiliations: Universidad Central del Caribe, Bayamon, Puerto Rico (Sanchez Perez); Department of Radiology, Cincinnati Children's Hospital, Ohio (AJ Towbin); Department of Radiology, University of Cincinnati College of Medicine, Ohio (AJ Towbin, Morgan); Department of Radiology, Phoenix Children's Hospital, Arizona (RB Towbin).

Published: October 1, 2024. https://doi.org/10.1016/10.37549/AR-D-24-0021

Figure 1. Axial (A) and coronal (B) contrast-enhanced CT of the abdomen shows a mass (arrows) arising from the tail of the pancreas. The mass compresses the splenic vein (arrowhead in A) and has a solid, enhancing component posteriorly and inferiorly (arrowhead in B).

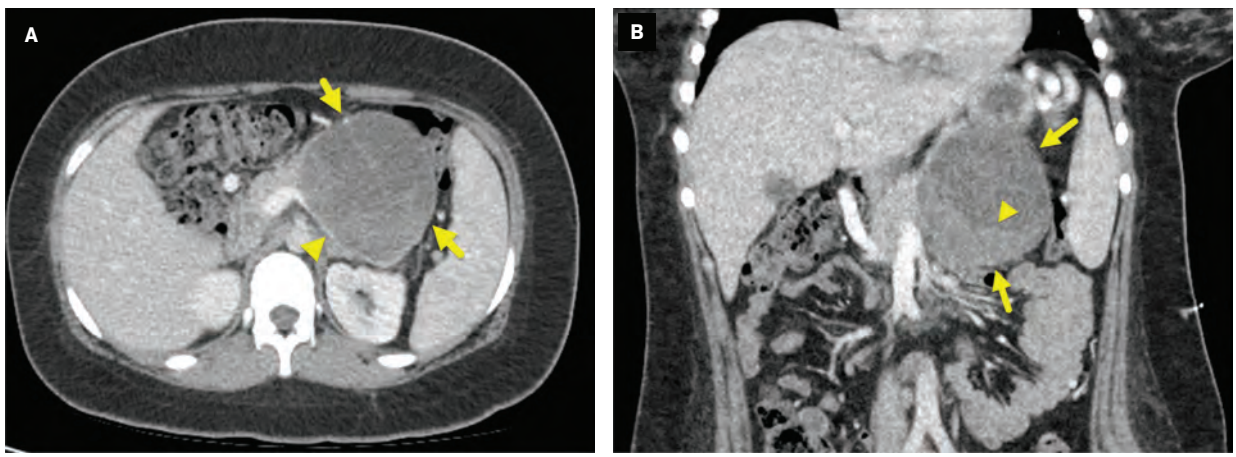

Figure 2. Axial T2-weighted MRI without (A) and with (B) fat suppression shows a heterogeneous pancreatic mass (arrow). The mass has layering fluid/debriswithin the cystic component (arrowhead in A), a heterogeneous posterior solid component, and does not contain fat. Axial T1-weighted dynamic spoiled gradient echo sequence (C) obtained 4 minutes after contrast administration shows mild enhancement (arrow) of the solid component of the mass. Diffusion-weighted sequence (b-value = 800) (D) shows restricted diffusion (arrow) in the enhancing portion of the mass.

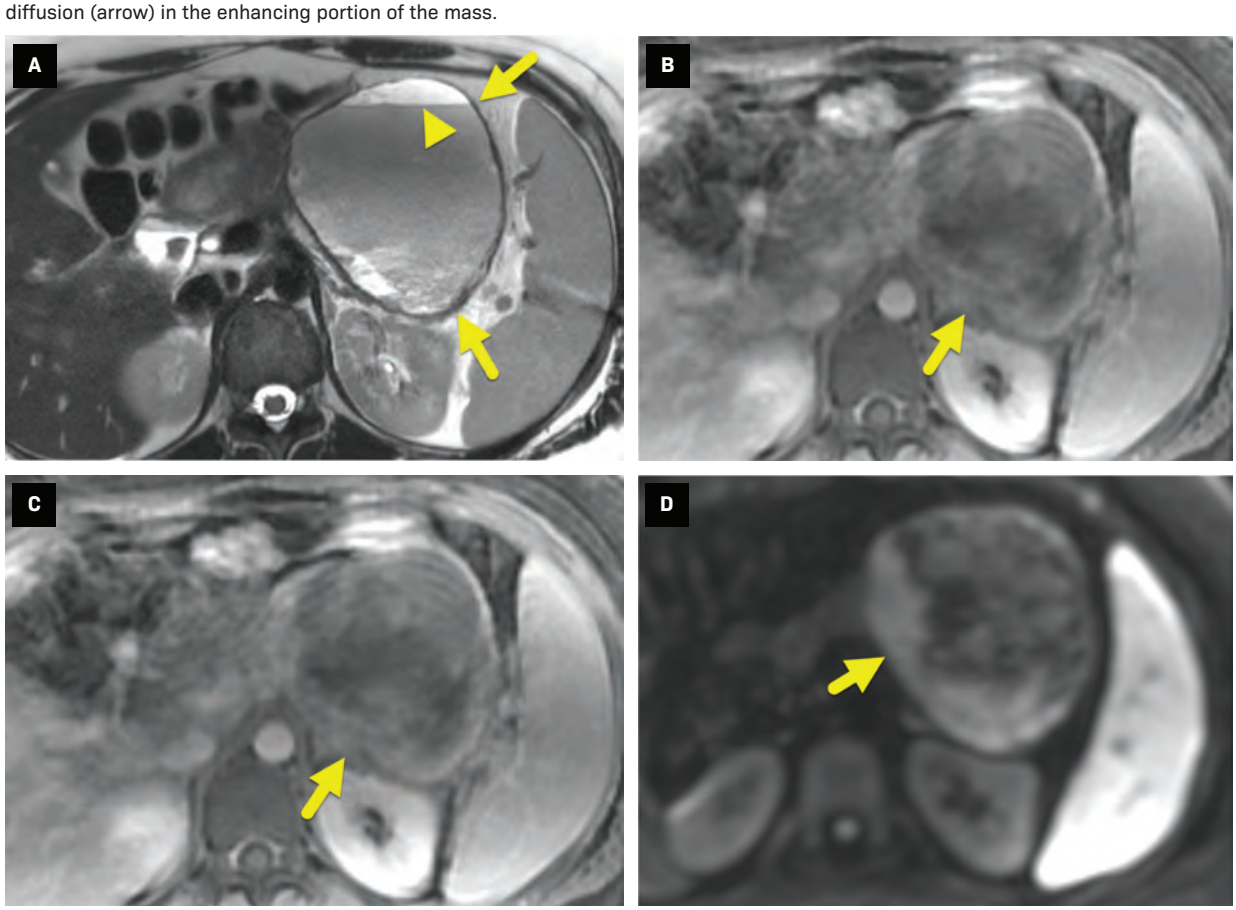

guided by endoscopic ultrasound (EUS).[3] Histological features of SPT include branching fragments with central capillaries and myxoid stroma. On microscopic examination, the cells are uniform and polygonal, with abundant cytoplasm containing oval, regular nuclei. Immunohistological markers have been used adjunctly for diagnosing SPTs of the pancreas. These tumors are strongly positive for vimentin, alpha-1 antitrypsin, and neuron-specific enolase.[3,4] Tumor cells from SPTs usually do not stain for chromogranin and synaptophysin, which help distinguish them from islet cell tumors. They usually do not stain for keratin, which can help distinguish SPTs from acinar carcinoma.[4] This is important as SPT is often considered in the differential diagnosis based on imaging characteristics, but it is uncommon.[4]

On imaging, SPT is characterized by hemorrhage and cystic degenerative change; it can be cystic, cystic and solid, or a solid mass. On ultrasound, SPT typically appears as large and well-defined, with capsular integrity.[1,4] On CT, it is typically well-encapsulated, with heterogeneous density and contrast enhancement of peripherally-located solid components.[1,4] On MRI, SPTs are usually heterogeneously hypointense on T1, and heterogeneously hyperintense on T2.[1,10] After contrast injection, there is patchy enhancement of internal components.[1,4] MRI is generally the imaging modality of choice as it can show hemorrhage, cystic degeneration, and integrity of tumor capsule, the classic features of pancreatic SPT.[4]

There is inconsistency in the literature regarding its most common location; some studies suggest that the body and tail of the pancreas are more common, whereas others have found that SPT occurs relatively equally in the head and tail .[1,4,9,10] The tumors are typically large at diagnosis, with an average diameter of 8cm.[9,10] A systematic analysis that collected studies performed before and after the year 2000 found that the average size at diagnosis had decreased while the number of cases of pancreatic SPT had increased.[10] These trends are thought to be due to earlier detection with improved imaging.

Solid pseudopapillary tumor typically has a good prognosis after surgical resection. However, malignant progression and fatal outcomes have been reported.[3,4] It is not clear what causes malignant or aggressive progression.[4]

Conclusion

An SPT of the pancreas is an exocrine parenchymal neoplasm characterized by cystic and/or solid components that usually affect young women of reproductive age. Patients most commonly present with abdominal pain and a palpable mass. Diagnosis is usually made using FNA guided by EUS.

These tumors are considered low-grade neoplasms with an overall good prognosis. Early recognition of characteristic imaging features on ultrasound, CT, and/or MRI can aid in diagnosis.

References

1) Weerakkody Y. Solid pseudopapillary tumor of the pancreas. Reference article, Radiopaedia.org. Accessed August 18, 2022. https://doi.org/10.53347/rID-16859

2) Shuja A, Alkimawi KA. Solid pseudopapillary tumor: a rare neoplasm of the pancreas. *Gastroenterol Rep (Oxf)*. 2014;2(2):145-149. doi:10.1093/gastro/gou006

3) Bardales RH, Centeno B, Mallery JS, et al. Endoscopic ultrasound-guided fine-needle aspiration cytology diagnosis of solid pseudopapillary tumor of the pancreas: a rare neoplasm of elusive origin but characteristic cytomorphologic features. *AM J Clin Pathol*. 2004;121(5):654-662. doi:10.1309/DKK2-B9V4-N0W2-6A8Q

4) Guo N, Zhou QB, Chen RF, et al. Diagnosis and surgical treatment of solid pseudopapillary neoplasm of the pancreas: analysis of 24 cases. *Can J Surg*. 2011;54(6):368-374. doi:10.1503/cjs.011810

5) Papavramidis T, Papavramidis S. Solid pseudopapillary tumors of the pancreas: review of 718 patients reported in English literature. *J Am Coll Surg*. 2005;200(6):965-972. doi:10.1016/j.jamcollsurg.2005.02.011

6) Yao J, Song H. A review of clinicopathological characteristics and treatment of solid pseudopapillary tumor of the pancreas with 2450 cases in Chinese population. *Biomed Res Int*. 2020;2020:2829647. doi:10.1155/2020/2829647

7) Yu P-F, Hu Z-H, Wang X-B, et al. Solid pseudopapillary tumor of the pancreas: a review of 553 cases in Chinese literature. *World J Gastroenterol*. 2010;16(10):1209-1214. doi:10.3748/wjg.v16.i10.1209

8) Law JK, Ahmed A, Singh VK, et al. A systematic review of solid-pseudopapillary neoplasms: are these rare lesions? *Pancreas*. 2014;43(3):331-337. doi:10.1097/MPA.0000000000000061

9) Wu J, Mao Y, Jiang Y, et al. Sex differences in solid pseudopapillary neoplasm of the pancreas: a population-based study. *Cancer Med*. 2020;9(16):6030-6041. doi:10.1002/cam4.3180

10) Speer AL, Barthel ER, Patel MM, Grikscheit TC. Solid pseudopapillary tumor of the pancreas: a single-institution 20-year series of pediatric patients. *J Pediatr Surg*. 2012;47(6):1217-1222. doi:10.1016/j.jpedsurg.2012.03.026

Cerebral Venous Sinus Thrombosis

Rayan W. Yahia, MD; Richard B. Towbin, MD; Carrie M. Schaefer, MD; Daniel Morgan, DO; Alexander J. Towbin, MD

Case Summary

A teenager with a surgical history of craniotomy for craniosynostosis and a medical history of menorrhagia requiring oral contraceptives presented with 1 month of worsening frontal, parietotemporal, and occipital headaches. Initially, the headaches occurred only in the morning but progressed to occurring throughout the day. The patient noted that the headaches improved while lying flat and worsened with Valsalva, increased activity, and bending over.

Imaging Findings

Noncontrast head CT (Figure 1) showed asymmetric, increased attenuation in the left transverse and sigmoid sinuses extending to the superior aspect of the left internal jugular vein.

Subsequent MRI and magnetic resonance venography (MRV) of the brain (Figure 2) confirmed the thrombus within the left transverse and sigmoid sinuses extending from the origin of the left internal jugular vein to the level of C5. There was a corresponding T1 hyperintensity, minimal T2 hyperintensity, and moderate magnetic susceptibility effect in these regions, consistent with an intraluminal thrombus.

Diagnosis

Cerebral venous sinus thrombosis (CVST).

The differential diagnosis for new-onset headaches includes primary and secondary causes. Primary causes include tension, migraine, and cluster headaches.[1] Secondary headaches can stem from intracranial tumors, hemorrhage, venous sinus thrombosis, increased intracranial pressure, and trauma.[2]

Discussion

In adults, the annual incidence of CVST is estimated to be 5 cases per million.[3] It is more common in women.[3] This differs from children, where the annual incidence is approximately 7 cases per million.[4] Pediatric CVST occurs most commonly in neonates. There is no gender difference in incidence in children.[4]

CVST may occur because of local or systemic factors. Local factors that impact venous sinus blood flow include trauma, infection, and neoplasm. Systemic factors include medications such as oral contraceptives and prothrombotic conditions or states. CVST has no known cause in up to 25% of patients.[5]

Headache is the most common presenting symptom in up to 95% of patients.[5] Other nonspecific signs and symptoms may include lethargy, mental status changes, and vomiting. Focal neurological deficits can also occur. These are more common in patients with parenchymal changes on imaging.[5]

In CVST, the increased venous pressure and subsequent disruption of the blood-brain barrier lead to extravasation of fluid, causing cerebral edema.[6] If the elevated venous pressure exceeds arterial pressure, ischemia or hemorrhagic stroke can occur.[6] Depending on its location, the thrombus can prevent reabsorption of cerebrospinal fluid from the periventricular regions.[6]

The superficial venous system is most commonly affected, with the superior sagittal and transverse sinuses serving as primary locations. The internal jugular and cerebral veins are also common sites of thrombosis.[6]

Diagnosis is made via imaging, and the initial imaging modality of choice depends on the population. In neonates, transfontanelle US is often the first-line imaging technique used due to its noninvasive nature and bed-side portability.[7] This is usually followed by brain CT or MRI to determine the extent

Affiliations: University of California, Riverside-School of Medicine, Los Angeles, California (Yahia); Department of Radiology, Phoenix Children's Hospital, Phoenix, Arizona (RB Towbin, Schaefer); Department of Radiology, University of Cincinnati College of Medicine, Cincinnati, Ohio (Morgan, AJ Towbin); Department of Radiology, Cincinnati Children's Hospital, Cincinnati, Ohio (AJ Towbin).

Published: August 1, 2024. https://doi.org/10.1016/10.37549/AR-D-24-0016

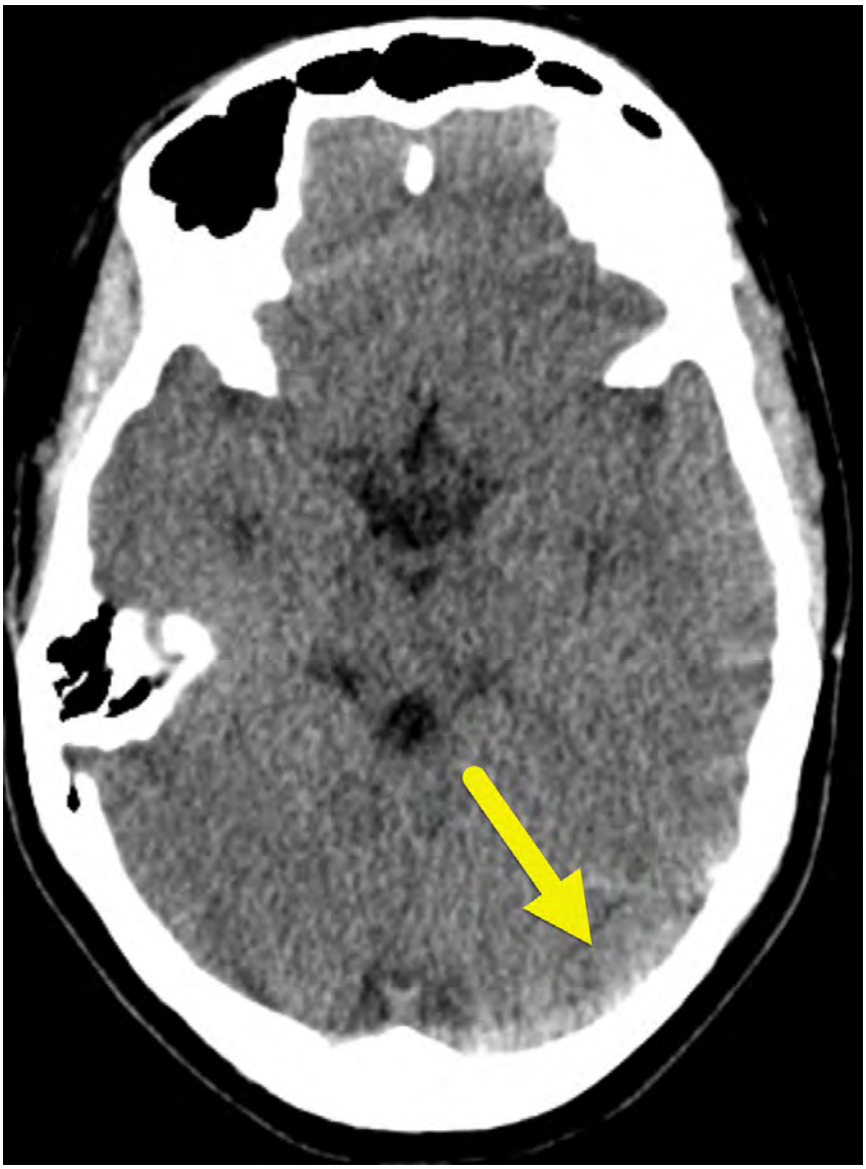

Figure 1. Noncontrast head CT showing asymmetric, increased density in the left transverse sinus (arrow).

of the thrombus and its impact. In children and adults, noncontrast head CT is typically the initial imaging modality. If the results are positive or equivocal with high clinical suspicion, a CT venogram or MRI/MRV is often obtained to determine the extent and impact of the thrombosis.[7]

CVST may be diagnosed by the "cord" sign or "empty delta" sign. The cord sign is used to describe the linear, expanded, hyperdense venous sinus on noncontrast CT. It is not a sensitive sign as it is only present in ~25%-56% of cases.[8] The empty delta sign occurs on postcontrast CT or MRI when the thrombus appears as a triangular-shaped filling defect surrounded by enhancing dural venous sinus or collateral channels, typically on axial imaging.[5] This sign is only present in approximately 29% to 35% of patients.[8]

On MRI, CVST may be first diagnosed with an absent or altered flow void.[8] The thrombus varies in signal intensity depending on its age. An acute CVST (1-5 d) appears isointense on T1-weighted images and hypointense on T2-weighted images, a subacute CVST (6-15 d) appears as hyperintense on both T1- and T2-weighted images, and a chronic CVST (>15 d) is isointense on T1-weighted images and iso/hyperintense on T2-weighted images.[10] MRI can also detect associated findings such as sinusitis, empyema, brain parenchymal abnormalities near the site of thrombus (~40%-60%), parenchymal hemorrhages (~30%-35%), and - less commonly - gyral edema/enhancement, diffuse edema,

Figure 2. Axial susceptibility-weighted image (A) shows moderate magnetic susceptibility effect in the left transverse sinus (arrow). There is also magnetic susceptibility effect in veins along the left side of the tentorium (arrowhead). Axial T1-weighted postcontrast fat-suppressed images at the level of the transverse sinus (B) and foramen magnum (C) show an intraluminal filling defect (arrow) within the left transverse sinus extending to the left internal jugular vein (C). In the sagittal T1-gradient echo postcontrast image (D), the intraluminal filling defect is surrounded by contrast, giving a form of the "empty delta sign." Coronal maximum intensity slab image (E) from the time of flight MRV highlights normal flow-related enhancement in the right transverse sinus (dashed arrow) extending to the right internal jugular vein. No flow-related enhancement is seen on the left owing to the sinus venous thrombosis.

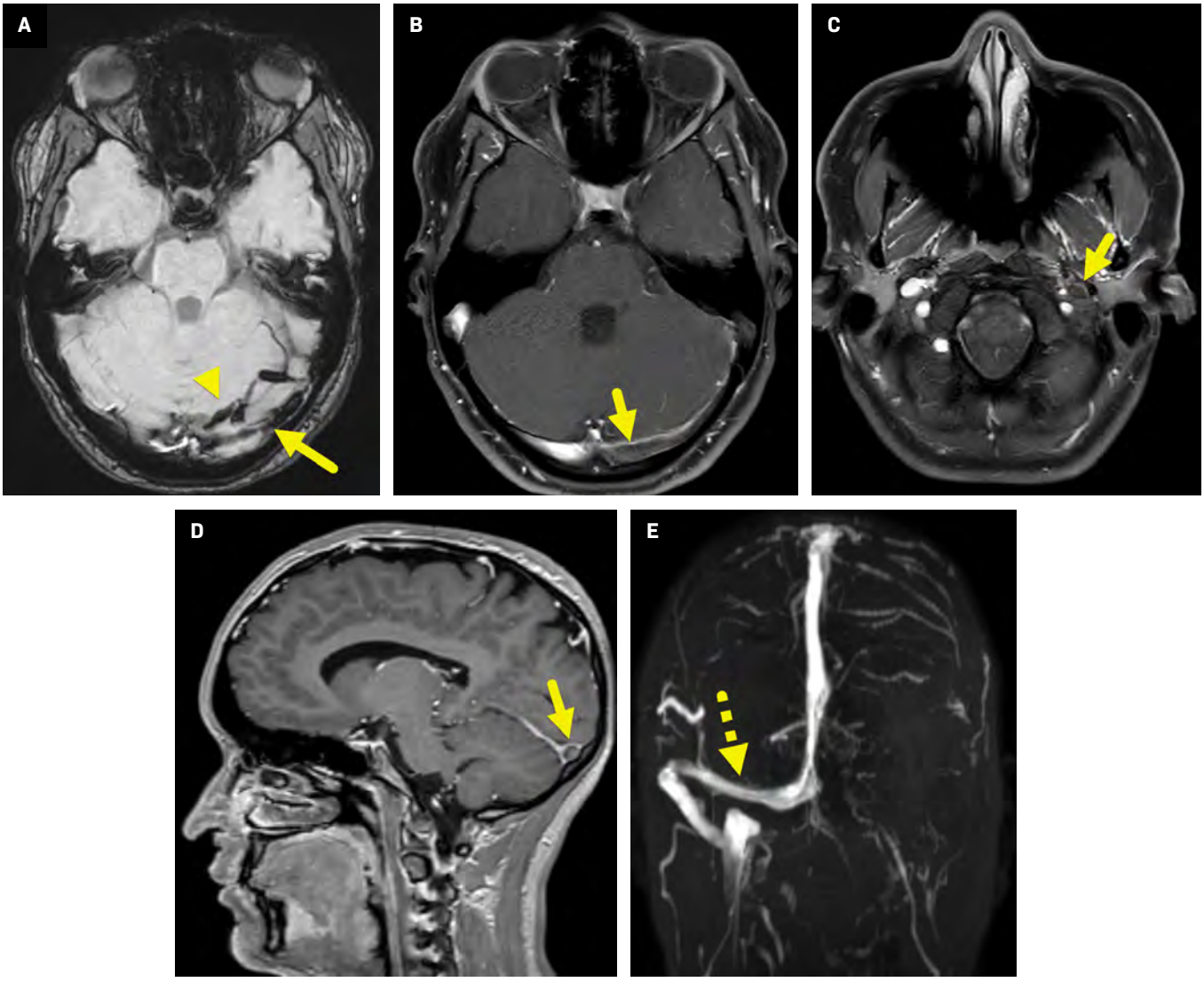

and decreased size of ventricles secondary to mass effect.[8]

The treatment for CVST is typically divided into acute phase and chronic phase. During the acute phase, treatment depends on the condition's severity. Patients with new focal neurological deficits should be considered for thrombolysis or endovascular thrombectomy if feasible.[8] Both acute and chronic phases warrant anticoagulation.[8]

Conclusion

CVST is a rare disorder more common in the pediatric population, especially in neonates. Presenting signs and symptoms are nonspecific and include headache, lethargy, altered mentation, vomiting, or focal neurological deficits. Imaging is crucial for diagnosing and determining CVST location. Treatment typically involves anticoagulation, thrombolysis, and/or endovascular thrombectomy.

References

1) Lipton RB, Bigal ME, Steiner TJ, Silberstein SD, Olesen J. Classification of primary headaches. *Neurology*. 2004;63(3):427-435. doi:10.1212/01.wnl.0000133301.66364.9b

2) Clinch CR. Evaluation of acute headaches in adults. *Am Fam Physician*. 2001;63(4):685-692.

3) Coutinho JM, Zuurbier SM, Aramideh M, Stam J. The incidence of cerebral venous thrombosis: a cross-sectional study. *Stroke*. 2012;43(12):3375-3377. doi:10.1161/STROKEAHA.112.671453

4) Suppiej A, Gentilomo C, Saracco P, et al. Paediatric arterial ischaemic stroke and cerebral Sinovenous thrombosis. *Thromb Haemost*. 2015;113(06):1270-1277. doi:10.1160/TH14-05-0431

5) Leach JL, Fortuna RB, Jones BV, Gaskill-Shipley MF. Imaging of cerebral venous thrombosis: current techniques, spectrum of findings, and diagnostic pitfalls. *RadioGraphics*. 2006;26 Suppl 1:S19-41; . doi:10.1148/rg.26si055174

6) Schaller B, Graf R. Cerebral venous infarction: the pathophysiological concept. *Cerebrovasc Dis*. 2004;18(3):179-188. doi:10.1159/000079939

7) Capecchi M, Abbattista M, Martinelli I. Cerebral venous sinus thrombosis. *J Thromb Haemost*. 2018;16(10):1918-1931. doi:10.1111/jth.14210

8) Canedo-Antelo M, Baleato-González S, Mosqueira AJ, et al. Radiologic clues to cerebral venous thrombosis. *RadioGraphics*. 2019;39(6):1611-1628. doi:10.1148/rg.2019190015